

## Excitonic properties of armchair graphene nanoribbons from exact diagonalization of the Hubbard model

This article has been downloaded from IOPscience. Please scroll down to see the full text article.

2012 New J. Phys. 14 053047

(<http://iopscience.iop.org/1367-2630/14/5/053047>)

View [the table of contents for this issue](#), or go to the [journal homepage](#) for more

Download details:

IP Address: 2.234.120.170

The article was downloaded on 13/03/2013 at 13:07

Please note that [terms and conditions apply](#).

## Excitonic properties of armchair graphene nanoribbons from exact diagonalization of the Hubbard model

Jessica Alfonsi<sup>1</sup> and Moreno Meneghetti

Nanostructures for Optics Laboratory, Department of Chemical Sciences,  
University of Padova, Padova, Italy  
E-mail: [jessica.alfonsi@unipd.it](mailto:jessica.alfonsi@unipd.it)

*New Journal of Physics* **14** (2012) 053047 (10pp)


Received 27 January 2012

Published 31 May 2012

Online at <http://www.njp.org/>

doi:10.1088/1367-2630/14/5/053047

**Abstract.** We report on excitonic spectra of armchair graphene nanoribbons (AGNRs) obtained from a full many-body exact diagonalization of the Hubbard model within low and intermediate correlation regimes and with a complete characterization of the spin multiplicity of the calculated eigenstates. Our results allow us to group these systems into three different families according to the sequence of the one- and two-photon allowed states and the magnitude of the respective optical oscillator strengths within the investigated correlation regime. The oscillator strengths for the one-photon allowed transitions are found to be lower than those obtained previously for zigzag semiconducting single-walled carbon nanotubes, pointing out a qualitatively different photophysical behaviour of AGNRs.

 Online supplementary data available from [stacks.iop.org/NJP/14/053047/mmedia](http://stacks.iop.org/NJP/14/053047/mmedia)

<sup>1</sup> Author to whom any correspondence should be addressed.

**Contents**

|                                  |          |
|----------------------------------|----------|
| <b>1. Introduction</b>           | <b>2</b> |
| <b>2. Method</b>                 | <b>3</b> |
| <b>3. Results and discussion</b> | <b>5</b> |
| <b>4. Conclusions</b>            | <b>8</b> |
| <b>Acknowledgments</b>           | <b>9</b> |
| <b>References</b>                | <b>9</b> |

**1. Introduction**

Boosted by the recent progress in the synthesis and isolation of single graphene layers [1–3], graphene nanoribbons (GNRs) have attracted much attention because of the possibility of opening a tunable electronic band gap in their electronic spectrum by changing their edge structure and ribbon width. This would allow to overcome the gaplessness of graphene, which is one of the main limitations preventing its application in electronic devices [4, 5]. Over the last few years, progress in the bottom-up fabrication of GNRs has allowed high-quality stripes of less than 10 nm width to be obtained, whose band gap can be exploited to make field-effect transistors [6–9]. Until recently the electronic structure of GNRs with proper boundary conditions at the edges has mostly been investigated with tight-binding (TB) methods for  $\pi$ -electrons [10], the  $k \cdot p$  two-dimensional (2D) Weyl–Dirac equation for free massless particles with the Fermi velocity ( $10^6 \text{ m s}^{-1}$ ) playing the role of an effective speed of light [11] or *ab initio* density functional calculations [12], which have all been recently surveyed in several excellent theoretical reviews [13–16]. GNRs are usually classified according to their type of edge, either zigzag or armchair, even though disordered or more complicated regular types of edges are possible. The electronic properties of armchair nanoribbons (AGNRs) are simpler than those of zigzag ones because of the absence of zero-energy localized states. Furthermore, they can be related to the electronic structure of zigzag single-walled carbon nanotubes (ZSWCNTs) since the van Hove singularities occur at the centre of the Brillouin zone [17–19].

Although both the TB and the Weyl–Dirac equation predict that armchair GNRs with pristine edges may be either semiconducting or metallic according to their width (oscillating gap), it is now generally accepted also on the basis of *ab initio* and mean-field Hubbard model results that AGNRs are always semiconducting, since the metallic state is unstable against bond deformations at the edges, electron–electron interactions and longer-range hoppings, as discussed by Cresti *et al* [20] and Rozhkov *et al* [21] in their reviews.

Optical selection rules and analytical expressions for the electron–light interaction matrix elements obtained on the basis of the TB model for both armchair and zigzag GNRs and different light polarizations (either parallel or perpendicular to the GNR edges) have also recently been reported [22, 23] and discussed in relation to the previously determined optical selection rules for SWCNTs [24, 25].

Besides the aforementioned studies based on independent-particle approximation, there have also been several attempts to include many-body effects in GNRs at a further level of theory, since electron–electron interactions are expected to be enhanced in low-dimensional systems. Following closely the roadmap adopted for SWCNTs, many-body effects in GNRs have been investigated with many-body perturbation theory *ab initio*

GW–Bethe–Salpeter-based methods [26, 27], Pariser–Parr–Pople effective model Hamiltonians for  $\pi$ -electrons incorporating longer-range Coulomb interactions [28, 29] and Hubbard model-based approaches, either within the mean-field approximation applied to investigate the edge-state in zigzag ribbons [17] or with configuration interaction calculations applied to both armchair and zigzag edge geometry [30]. The validity of mean-field approximation when applying the Hubbard model to graphene-based systems has also been recently debated [31–34], in view of the low–intermediate value for the Hubbard correlation coupling strength ( $1 < U/t < 2.2$ ) which seems plausible for these systems.

In this work, we apply the small crystal approach (SCA) to perform an exact diagonalization (ED) of the Hubbard Hamiltonian in order to obtain the full many-body description of the electronic excitation spectrum of AGNRs of different widths. The SCA allows us to use a minimal number of sites to sample the most relevant  $k$ -points in the Brillouin zone that are critical for the electronic density of states (DOS) and optical oscillator strength of the system under investigation. Previously, we applied this method to obtain the excitonic structure of medium diameter semiconducting-like zigzag SWCNTs and investigated its profile as a function of the Hubbard correlation coupling strength [36, 37]. Following the same strategy, we choose two-leg ladder models mimicking AGNRs of different widths and consider optical transitions with light polarization along the nanoribbon edges. In this way, we sample a set of  $k$ -points equivalent to those considered for the van Hove singularities in the electronic DOS and longitudinal optical matrix elements of zigzag SWNTs. By performing ED calculations in the low–intermediate correlation regime for different values of the total spin  $S_z$ , we are able to provide a detailed description of the lowest-energy optically active (bright) and inactive (dark) excitons within a full many-body picture, which has not been presented so far in the GNR literature. Our results for the allowed transitions and related optical oscillator strength versus  $U/t$  point out a qualitatively different behaviour than that found for semiconducting SWCNTs and allow us to group AGNRs into three different families according to the sequence of one- and two-photon transitions in the electronic spectrum and the magnitude of the corresponding optical matrix elements within the considered correlation regime.

## 2. Method

Figure 1 shows the geometrical structure of a GNR with armchair geometry. Periodic boundary conditions are applied along the direction parallel to the edges, while the width of the armchair ribbon is given by the number  $N$  of dimer lines containing  $N$  A-type and  $N$  B-type carbon atoms. Following the traditional nomenclature for GNRs [12], we consider in this work AGNRs with  $4 \leq N \leq 7$ , with  $2N$  sites in their unit cell. One recalls that the 7-AGNR structure has also been recently obtained from aromatic precursors and investigated by both scanning tunnelling microscopy and Raman spectroscopy [9].

We study the  $N$ -AGNRs with brick-type lattices (i.e. with periodic ladders) which are topologically equivalent to the structures of AGNRs [12, 20]. Moreover, considering periodic boundary conditions along the direction parallel to the nanoribbon edges, we sample the  $k_{\parallel} = 0$  states in the GNR Brillouin zone. The brick-type lattice, made of coupled chains, can thus be folded into a two-leg ladder with  $N$  rungs and a unique value  $t$  for all nearest-neighbour hopping parameters in the Hamiltonian (see figure 3 in [12]). We consider the usual form for the Hubbard

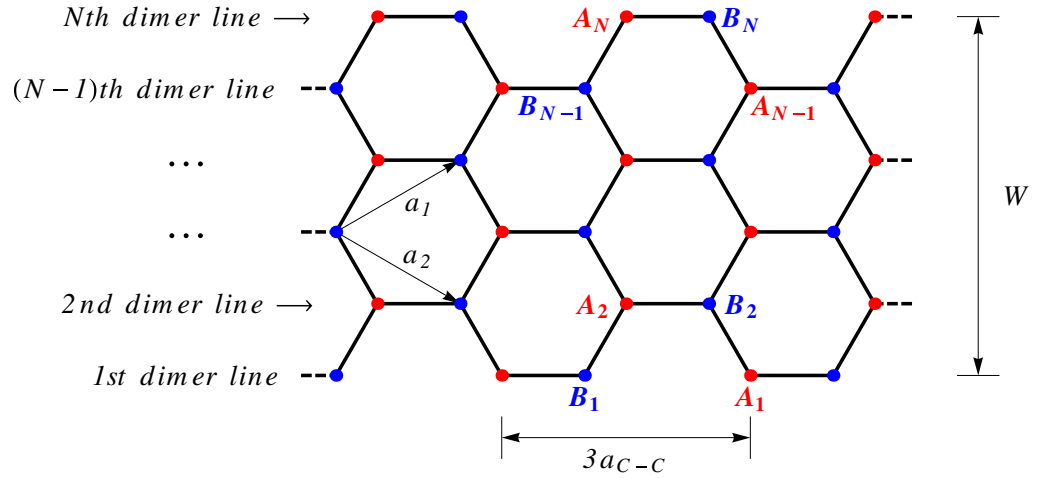


**Figure 1.** An armchair nanoribbon of width  $W$  with  $N$  dimer lines. A (B)-type atoms are shown in red (blue), respectively. Equivalent atoms on the honeycomb lattice are mapped by the  $a_1$  and  $a_2$  basis vectors.

Hamiltonian for  $\pi$ -electrons

$$H^{2D} = -t_\pi \sum_{\langle i,j \rangle, \sigma} (c_{i,\sigma}^\dagger c_{j,\sigma} + \text{h.c.}) + U \sum_i n_{i,\uparrow} n_{i,\downarrow}, \quad (1)$$

where  $i$  and  $j$  are site indices,  $\langle i, j \rangle$  are all pairs of first nearest-neighbour sites,  $c_{i,\sigma}^\dagger$  and  $c_{i,\sigma}$  are the electron creation and annihilation operators,  $n_{i,\sigma} = c_{i,\sigma}^\dagger c_{i,\sigma}$  is the number of electrons on site  $i$  with spin  $\sigma$ ,  $t_\pi$  and  $U$  are the nearest-neighbour hopping parameter and the on-site Coulomb repulsion parameter between two electrons with opposite spins, respectively. We recall that within this Hamiltonian the on-site Coulomb interaction  $U$  must be considered an effective parameter, whose value for half-filled systems with non-small values of the interactions can be taken as equivalent to  $U^{\text{eff}} = U - V_1$ , where  $V_1$  is the first nearest-neighbour Coulomb interaction in the extended Hubbard models [29, 36]. Thus the (effective)  $U$  parameter also implicitly takes into account longer-range Coulomb interactions in the limit of static screening, as discussed by Wehling *et al* [35].

The one-photon optical spectral function of the AGNR is calculated according to the Lehmann representation

$$I(E) = \sum_m |\langle \psi_m | v_{\parallel}^{2D} | \psi_{\text{GS}} \rangle|^2 \delta(E + E_{\text{GS}} - E_m), \quad (2)$$

where  $E_{\text{GS}}$  is the ground-state (GS) energy of the system and  $E_m$  the energy of any other eigenstate  $|\psi_m\rangle$  obtained from ED of the Hubbard Hamiltonian and  $v_{\parallel}^{2D}$  is the velocity operator for light polarization along the GNR edges, which can be expressed concisely as

$$v_{\parallel}^{2D} = -\frac{it_\pi}{\hbar} \sum_{\langle i,j \rangle, \sigma} (c_{i,\sigma}^\dagger c_{j,\sigma} - c_{j,\sigma}^\dagger c_{i,\sigma})_{\parallel}. \quad (3)$$

The extended expressions of  $v_{\parallel}^{2D}$  for each of the considered AGNRs are given in the supporting information<sup>2</sup>. This operator obeys the selection rule for the azimuthal band quantum number  $\mu$ , namely  $\Delta\mu = 0$  for interband transitions in AGNRs with light polarization along the nanoribbon edges [22, 24]. This implies that vertical transitions occur between van Hove singularities belonging to the same AGNR band quantum number in the TB picture (supplementary figure 2)<sup>2</sup>. Here we made the choice of considering only the case of polarization along the ribbon edges, since in armchair GNRs strong depolarization effects are known to quench the optical absorption for polarization perpendicular to the edges, contrary to zigzag GNRs which do not seem to display this behaviour for perpendicular polarization [22]. We recall that this formulation follows the same basic assumptions as those formerly outlined for zigzag SWCNTs [36, 37].

The two-photon allowed eigenstates are recognized from the matrix elements of  $v_{\parallel}^{2D}$  considering as the starting states the one-photon allowed eigenstates obtained from equation (2). We consider a half-filled system with  $n$  electrons distributed over  $n = 2N$  sites. In the case of states with spin quantum number  $S_z = 0$ , the size of the basis set and hence the dimension of the matrix to be diagonalized is  $D = [n!/(n_{\uparrow}!n_{\downarrow}!)]^2$ , where  $n_{\uparrow}$  and  $n_{\downarrow}$  are the numbers of spin-up and spin-down electrons, respectively, with  $n_{\uparrow} = n_{\downarrow} = N$ . In order to perform ED, we adopted an iterative diagonalization scheme based on the Lanczos algorithm, as implemented in the ALPS libraries [38], and an additional matrix-free strategy with shared-memory parallelization [39] to speed-up the diagonalization of the larger systems with 12 and 14 sites mimicking the 6- and 7-AGNRs, respectively. ED calculations were performed for several values of the  $U/t$  correlation coupling strength and spin quantum number  $S_z = (n_{\uparrow} - n_{\downarrow})/2$  in order to discriminate the obtained eigenstates on the basis of their spin multiplicity in addition to their one- and two-photon spectral activity.

### 3. Results and discussion

In figure 2 we report the one- and two-photon transitions for AGNRs with  $N = 4, 5, 6, 7$  in the low and intermediate correlation regimes for  $0 < U/t < 4$ . For the case  $U/t = 0$  we verified the TB results for the allowed interband electronic transition energies and for the metallicity condition,  $N = 3p + 2$ , with  $p$  an integer, for 5-AGNR. For the other ribbons with  $N = 3p$  (6-AGNR) and  $N = 3p + 1$  (4- and 7-AGNR) we verified the semiconducting behaviour. When electronic correlations are taken into account ( $U/t > 0$ ) one can see that a different behaviour is still present for the three types of ribbons, but for 5-AGNR the metallic behaviour is no longer found because of the lifting of the K-point degeneracy. For semiconducting AGNRs belonging to the  $N = 3p + 1$  family, namely 4- and 7-AGNRs, in the very low correlation regime  $U/t \ll 1$ , both one-photon active states ES11 and ES22 (following the usual notation adopted for SWCNTs) occur at lower energies than the two-photon active states, whereas for the semiconducting  $N = 3p$  (6-AGNR) the ES22 transition is found above the first two-photon active transition energy. However, if we consider that GNRs are in the intermediate–low correlation regime  $1 \leq U/t \leq 2$ , at least one two-photon allowed transition is always found between ES11 and ES22 for all the three AGNR families. As shown in figure 2, both ES11 and ES22 transitions in AGNRs run almost parallel to each other in the considered correlation range, and we do not find the crossing behaviour found for zigzag SWCNTs [36, 37]. Using

<sup>2</sup> Online supplementary data available from [stacks.iop.org/NJP/14/053047/mmedia](http://stacks.iop.org/NJP/14/053047/mmedia).

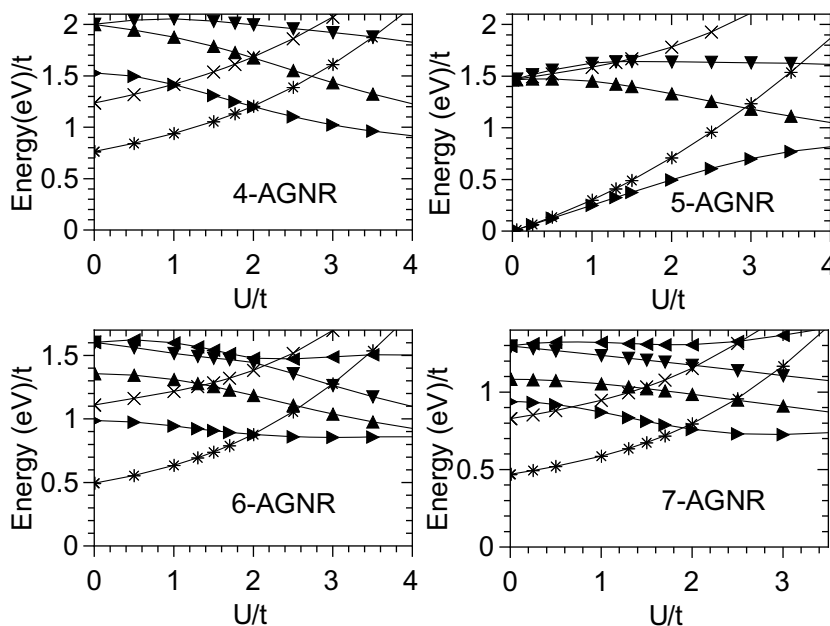


**Figure 2.** Transition energies versus  $U/t$  for the considered  $N$ -AGNRs with  $N = 4, 5, 6, 7$ . Symbol legends: (\*) first one-photon bright state E11; (x) second one-photon bright state E22; two-photon states are denoted by triangles.

$t_\pi = 2.6$ – $2.8$  eV, typical of graphene [31, 35], we obtain one-photon transition energies ES11 and ES22 of the same order of those previously computed by GW Bethe–Salpeter methods [26, 27] or by the PPP Hamiltonian [28, 29] for the corresponding families. As also discussed by Ezawa [10], taking into account the bond deformation at the nanoribbon edge with a different hopping parameter for the exposed sites and additional different on-site energy does not alter the qualitative feature of the excitonic spectrum computed for the pristine AGNRs in the intermediate correlation regime.

We find that the optical oscillator strengths versus  $U/t$  of ES11 (ES22) transition is always increasing (decreasing), with the correlation strength for AGNR with  $N = 3p$  and  $N = 3p + 1$ , whereas for  $N = 3p + 2$  (5-AGNR) both transitions show a constantly decreasing oscillator strength in the range  $U/t > 1$  (figure 3). In the latter case, one can also see that in the correlation range  $1 \leq U/t \leq 2$ , the optical oscillator strengths for both transitions are very close in magnitude, whereas for  $N = 3p, 3p + 1$  the intensity of the ES11 transition is on average 1.5–3 times as strong as the ES22 one. This finding agrees with the observation of Prezzi *et al* [27] that the luminescence properties are strongly family dependent, although our trends point out for a significantly different luminescence behaviour for  $N = 3p + 2$  (5-AGNR) only.

In general, one finds that the magnitudes of the  $t^2$ -normalized ES11 and ES22 optical oscillator strengths of AGNRs are always lower than those calculated for zigzag semiconducting SWNTs in the  $1 \leq U/t \leq 2$  regime from an ED calculation on a cluster model with the same number of sites (table 1).

We found a different behaviour for the two-photon oscillator strengths with respect to zigzag SWNTs [37]. In nanotubes the oscillator strength shows a drop of about two orders of magnitude when  $U/t$  crosses 1.8. This is not found for AGNRs, which show a smooth behaviour in the entire explored correlation regime.

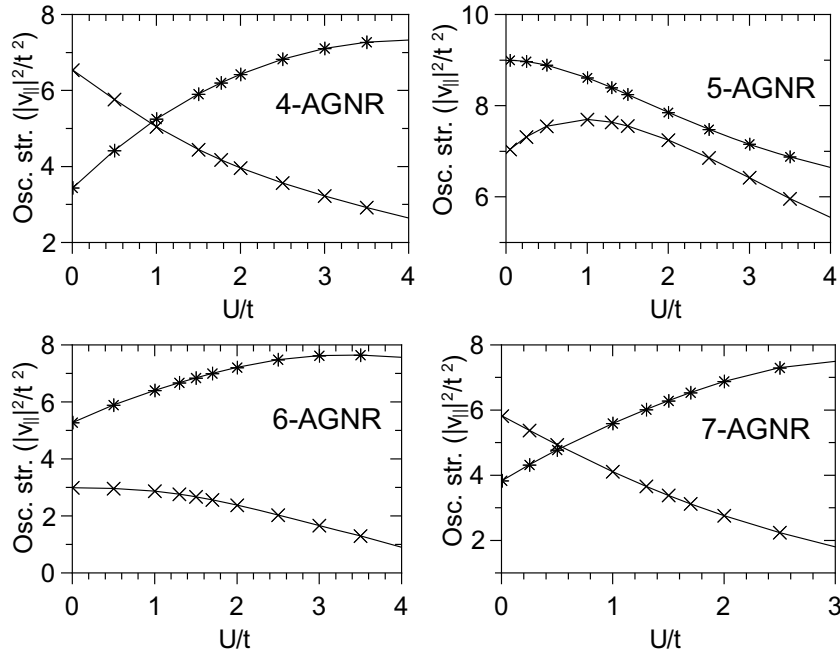


**Figure 3.** Oscillator strengths versus  $U/t$  for the considered  $N$ -AGNRs with  $N = 4, 5, 6, 7$ . Symbol legends: (\*) first one-photon bright state E11; (x) second one-photon bright state E22.

**Table 1.** Comparison of ES11 and ES22 oscillator strengths in units of  $|v||^2/t^2$  for a (7, 0) SWNT and a 7-AGNR obtained from ED of a cluster with 14 sites in the low-intermediate correlation regime.

| $U/t$ | 7-AGNR ES11 | (7, 0) ES11 | 7-AGNR ES22 | (7, 0) ES22 |
|-------|-------------|-------------|-------------|-------------|
| 1.0   | 5.6         | 12.4        | 4.1         | 10.5        |
| 1.3   | 6.0         | 12.7        | 3.7         | 11.4        |
| 1.5   | 6.3         | 12.7        | 3.4         | 11.7        |
| 1.7   | 6.5         | 12.7        | 3.1         | 11.9        |
| 2.0   | 6.9         | 12.5        | 2.8         | 12.2        |

In figure 4, we report the excitonic fine structure around the lowest bright exciton  $|B\rangle$  related to the ES11 transition. The presence of dark states below and above the first bright state influences the photoemission dynamics and yield.

Dark states showing two-photon absorption activity are calculated in the considered correlation regime above the lowest bright exciton state for all AGNRs with the exception of 5-AGNR, which shows a two-photon active dark state immediately below the ES11 transition. This different behaviour of the  $N = 3p + 2$  AGNR confirms the observation of Prezzi *et al* [27] that the presence of low-energy dark excitons in GNRs is dependent on the family. However, our results reported in figure 4 highlight almost similar low-energy excited-state structures for  $N = 3p$  and  $3p + 1$  AGNRs.

By changing the light polarization from parallel to perpendicular to the AGNR edge, we also verified that it is possible to activate the singlet dark states in the entire explored correlation



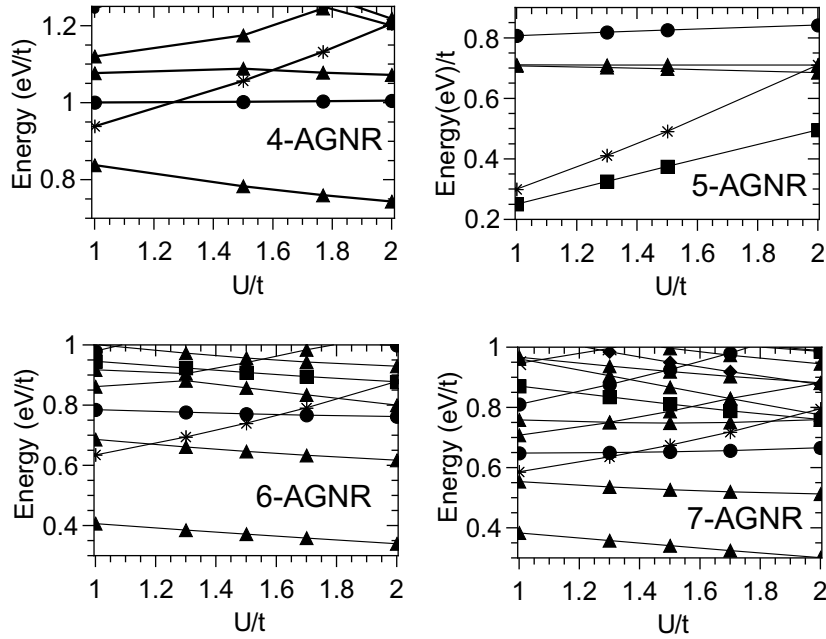


**Figure 4.** Dependence on the correlation strength  $U/t$  of the transition energies of the dark states in the proximity of the E11 transition from ED of the considered  $N$ -AGNRs with  $N = 4, 5, 6, 7$ . Symbol legends: (\*) bright (singlet, odd-parity) exciton  $|B\rangle$ ; (■) two-photon allowed (singlet, even-parity) dark excitons; (●) singlet dark excitons; (▲) triplet dark excitons; and (◆) quintuplet dark excitons.

regime, in agreement with the results reported for the GW–Bethe–Salpeter correlation regime by Louie *et al* [26] and Prezzi *et al* [27].

A feature in common with SWCNTs [37], for the  $N = 3p, 3p + 1$  AGNRs, is the presence of dark triplet and singlet states close to  $|B\rangle$ . These states can act as a population sink for the nearby bright exciton, which can consequently give delayed photoemission.

The presence of deep-lying triplet excited states can also be observed in figure 4 and is in accordance with the results obtained by Dutta *et al* [30], who reported that there are few dipole-forbidden high-spin excited states above the singlet GS. These states can play a significant role in quenching the radiative transition from the optically allowed excited state through a bottleneck mechanism, thus leading to a very low quantum efficiency in the luminescence spectroscopy of AGNRs.

#### 4. Conclusions

In summary, we have investigated the excitonic structure of pristine AGNRs of width less than 10 nm by ED of the Hubbard model for several two-leg ladder models mimicking ribbons with  $4 \leq N \leq 7$  dimer lines and with light polarized along the ribbon edges. By this full many-body approach applied to realistic systems, such as the 7-AGNRs fabricated by the most recent bottom-up techniques [9], we are able to investigate the effect of electronic correlations involved in direct interband optical transitions for several values of the electronic correlation parameter  $U/t$ . Our results in the very low correlation regime  $U/t \ll 1$  confirm that the

classification into three families provided for AGNRs by the single-particle picture still holds true even when electron–electron interactions are considered without approximations. Within the low–intermediate  $1 \leq U/t \leq 2$  correlation regime, which is considered to be appropriate for the graphene-based system, the magnitude of the optical oscillator strength of one-photon transitions for AGNRs is found to be lower than for single-walled carbon nanotubes, and two-photon absorption optical matrix elements do not show abrupt changes with increasing  $U/t$ . These results point out a qualitatively different behaviour in the photophysics of AGNRs when compared with semiconducting single-walled carbon nanotubes, which can be a crucial factor in the design of new carbon-based electronic devices.

### Acknowledgments

Financial support from the University of Padova (grant no. CPDR091818) is gratefully acknowledged. We also acknowledge the CINECA award HP10C4ZPOY under the ISCRA initiative for making available to us the high-performance computing system PLX and user support.

### References

- [1] Geim A K and Novoselov K S 2007 *Nature Mater.* **6** 183
- [2] Wu Y H, Yu T and Shen Z X 2010 *J. Appl. Phys.* **108** 071301
- [3] Cooper D R *et al* 2012 *ISRN Condens. Matter Phys.* **2012** 501686
- [4] Chen Z H, Lin Y M, Rooks M J and Avouris P 2007 *Physica E* **40** 228
- [5] Han M Y, Ozyilmaz B, Zhang Y B and Kim P 2007 *Phys. Rev. Lett.* **98** 206805
- [6] Kosynkin D V, Higginbotham A L, Sinitskii A, Lomeda J R, Dimiev A, Price B K and Tour J M 2009 *Nature* **458** 872
- [7] Jiao L Y, Zhang L, Wang X R, Diankov G and Dai H J 2009 *Nature* **458** 877
- [8] Jiao L, Wang X, Diankov G, Wang H and Dai H 2010 *Nature Nanotechnology* **5** 321
- [9] Cai J *et al* 2010 *Nature* **466** 470
- [10] Ezawa M 2006 *Phys. Rev. B* **73** 045432
- [11] Brey L and Fertig H A 2006 *Phys. Rev. B* **73** 235411
- [12] Son Y-W, Cohen M L and Louie S G 2006 *Phys. Rev. Lett.* **97** 216803
- [13] Neto C A H, Guinea F, Peres N M R, Novoselov K S and Geim A K 2009 *Rev. Mod. Phys.* **81** 109
- [14] Abergel D S L, Alpakov V, Berashevich J, Ziegler K and Chakraborty T 2010 *Adv. Phys.* **59** 261
- [15] Marconcini P and Macucci M 2011 *Riv. Nuovo Cimento* **34** 489
- [16] Wakabayashi K, Sasaki K I, Nakanishi T and Enoki T 2010 *Semicond. Technol. Adv. Mater.* **11** 054504
- [17] Fujita M, Wakabayashi K, Nakada K and Kusakabe K 1996 *J. Phys. Soc. Japan* **65** 1920
- [18] Zheng H, Wang Z F, Luo T, Shi Q W and Chen J 2007 *Phys. Rev. B* **75** 165414
- [19] Sasaki K I, Wakabayashi K and Enoki T 2011 *J. Phys. Soc. Japan* **80** 044710
- [20] Cresti A, Nemeč N, Biel B, Niebler G, Triozon F, Cuniberti G and Roche S 2008 *Nano Res.* **1** 361
- [21] Rozhkov A V, Giavaras G, Bliokh Y P, Freilikher V and Nori F 2011 *Phys. Rep.* **503** 77
- [22] Sasaki K I, Kato K, Tokura Y, Oguri K and Sogawa T 2011 *Phys. Rev. B* **84** 085458
- [23] Chung H C, Lee M H, Chang C P and Lin M F 2011 *Opt. Express* **19** 23350
- [24] Sasaki K I, Kato K, Tokura Y, Sogawa T and Saito R 2011 unpublished work (arXiv:1108.0041)
- [25] Hsu H and Reichl L E 2007 *Phys. Rev. B* **76** 045418
- [26] Yang L, Cohen M L and Louie S G 2007 *Nano Lett.* **7** 3112
- [27] Prezzi D, Varsano D, Ruini A, Marini A and Molinari E 2008 *Phys. Rev. B* **77** 041404
- [28] Gundra K and Shukla A 2011 *Phys. Rev. B* **83** 075413

- [29] Aryanpour K, Mazumdar S and Zhao H 2012 *Phys. Rev. B* **85** 085438
- [30] Dutta S, Lakshmi S and Pati S K 2008 *Phys. Rev. B* **77** 073412
- [31] Perfetto E, Cini M, Ugenti S, Castrucci P, Scarselli M, De Crescenzi M, Rosei F and El Khakani M A 2008 *J. Phys.: Conf. Ser.* **100** 052082
- [32] Feldner H, Meng Z Y, Honecker A, Cabra D, Wessel S and Assaad F F 2010 *Phys. Rev. B* **81** 115416
- [33] Yazyev O V 2010 *Rep. Prog. Phys.* **73** 056501
- [34] Palacios J J, Fernández-Rossier J, Brey L and Fertig H A 2010 *Semicond. Sci. Technol.* **25** 033003
- [35] Wehling T O, Şaşıoğlu E, Friedrich C, Lichtenstein A I, Katsnelson M I and Blügel S 2011 *Phys. Rev. Lett.* **106** 236805
- [36] Alfonsi J, Lanzani G and Meneghetti M 2010 *New J. Phys.* **12** 083009
- [37] Alfonsi J and Meneghetti M 2012 *J. Phys.: Cond. Matter* at press
- [38] Albuquerque A F *et al* 2007 *J. Magn. Magn. Mater.* **310** 1187  
Bauer B *et al* 2011 *J. Stat. Mech.* **2011** P05001
- [39] Schnack J, Hage P and Schmidt H-J 2008 *J. Comput. Phys.* **227** 4512